

Non-rigid Image Registration with $S\alpha S$ Filters

Shu Liao and Albert C.S. Chung

Lo Kwee-Seong Medical Image Analysis Laboratory,
Department of Computer Science and Engineering,
The Hong Kong University of Science and Technology, Hong Kong
liaoshu@cse.ust.hk, achung@cse.ust.hk

Abstract. In this paper, based on the $S\alpha S$ distributions, we design $S\alpha S$ filters and use the filters as a new feature extraction method for non-rigid medical image registration. In brain MR images, the energy distributions of different frequency bands often exhibit heavy-tailed behavior. Such non-Gaussian behavior is essential for non-rigid image registration but cannot be satisfactorily modeled by the conventional Gabor filters. This leads to unsatisfactory modeling of voxels located at the salient regions of the images. To this end, we propose the $S\alpha S$ filters for modeling the heavy-tailed behavior of the energy distributions of brain MR images, and show that the Gabor filter is a special case of the $S\alpha S$ filter. The maximum response orientation selection criterion is defined for each frequency band to achieve rotation invariance. In our framework, if the brain MR images are already segmented, each voxel can be automatically assigned a weighting factor based on the Fisher's separation criterion and it is shown that the registration performance can be further improved. The proposed method has been compared with the free-form-deformation based method, Demons algorithm and a method using Gabor features by conducting non-rigid image registration experiments. It is observed that the proposed method achieves the best registration accuracy among all the compared methods in both the simulated and real datasets obtained from the BrainWeb and IBSR respectively.

1 Introduction

Non-rigid medical image registration methods can be broadly classified into two categories: feature-based methods and intensity-based methods. The intensity-based non-rigid registration methods are the direct methods aiming to maximize or minimize the similarity functions defined between two images. Thirion [1] proposed the Demons algorithm to handle deformable registrations, Rueckert *et al.* [2] proposed free-form deformation (FFD) based method, and Vemuri *et al.* [3] suggested a level-set based deformable image registration method. The feature-based non-rigid registration methods model the image registration problem as a feature matching and optimization problem by extracting features such as surface landmarks, and shape information from the images. Various feature-based image registration methods have been proposed [4].

Gabor filter is a useful tool to capture the energy distributions of various frequency bands of an input image and has been applied to medical image registration as a feature extraction method [5]. Gabor filter is in fact a Gaussian kernel modulated by a complex sinusoid with a specific orientation. Therefore, the energy distributions of various frequency bands are characterized by the Gaussian kernel. However, as limited by the Gaussian kernel, Gabor filter is not a suitable choice to model non-Gaussian behavior, which occurs quite often in many practical applications [6]. In this paper, it is demonstrated that the energy distributions of different frequency bands of brain MR images often exhibit non-Gaussian heavy-tailed behavior. As such, Gabor filters cannot fully describe the characteristics of brain MR images. Another problem of the Gabor filter is that it is not rotation invariant. As pointed out in [7], rotation invariance is an important property for feature-based registration methods.

Therefore, we are motivated to propose the $S\alpha S$ filters as a feature extraction method for brain image non-rigid registration. The main contributions of this paper are as follows. First, the proposed $S\alpha S$ filters satisfactorily model the heavy-tailed behavior of the energy distributions of brain MR images. This can increase the registration accuracy. It is theoretically shown that the Gabor filter is a special case of the $S\alpha S$ filters. Second, in order to achieve rotation invariance, the maximum response orientation (MRO) selection criterion is defined and designed for each frequency band. It also reduces the computational burden for non-rigid image registration. Third, an optional training framework is proposed. If the segmentation results of input images are available, each voxel can be automatically assigned a weighting factor based on the Fisher's separation criterion (FSC). The larger is the weighting factor, the more important is the voxel during the registration process. It is shown that with this training step, the registration accuracy can be further improved. The proposed method has been evaluated by non-rigid registration experiments, and has been compared with the FFD, Demons algorithm and a method using Gabor features. It is shown that the proposed method achieves the best registration accuracy in both experiments on synthetic and real 3D image volumes.

2 Methodology

2.1 Feature Extraction with $S\alpha S$ Filters

Gabor filter, which was first proposed by Dennis Gabor [8], is a powerful mathematical tool for signal decomposition and image processing. The basic assumption under which the input image can be accurately described by Gabor filtered responses is that the energy distributions for various frequency bands follow the Gaussian distribution. However, many signals encountered in practical applications are non-Gaussian [6]. Using the Gaussian kernel to model non-Gaussian behavior usually results in significant performance degradation [6].

Figure 1(a) shows a T1 MR image slice obtained from the IBSR website¹, its normalized energy magnitude distributions of several frequencies are plotted in

¹ <http://www.cma.mgh.harvard.edu/ibsr/index.html>

blue bars from column 2 to column 4. In this example, it is observed that for brain MR images, the energy magnitude distributions of various frequency bands have non-Gaussian heavy-tailed behavior. Such behavior is more obvious in the mid and high frequency bands. Figures 1(b) to 1(d) show the best fitted Gaussian models obtained via maximum likelihood estimation for various frequency bands. It is observed that the heavy-tailed behavior cannot be satisfactorily modeled by the Gaussian kernel.

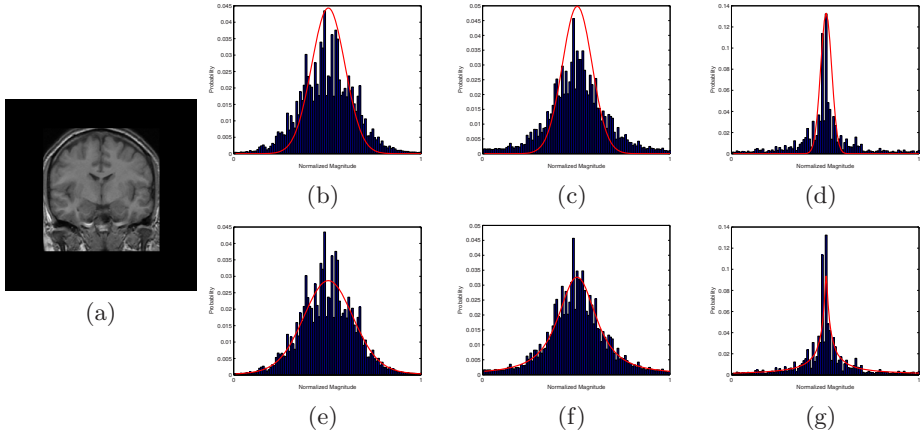


Fig. 1. Column 1 is an image slice from a 3D image volume obtained from the IBSR website. From column 2 to column 4: The blue bars represent the normalized energy magnitude distributions of the low frequency bands: 2.00 to 3.17, mid frequency bands: 3.17 to 5.04, high frequency bands: 5.04 to 9.00 (cycles/image) for the image in (a). Figures (b), (c) and (d) show the best fitted Gaussian models obtained via maximum likelihood estimation for different frequency bands (red curves). Figures (e), (f) and (g) show the best fitted $S\alpha S$ models obtained via maximum likelihood estimation for different frequency bands (red curves).

According to [6], symmetric Alpha-stable ($S\alpha S$) distribution is a powerful tool to model the heavy-tailed behavior as it has algebraic tails. Its characteristic function is given by Equation 1 [6]:

$$\varphi(t) = \exp\{jat - \gamma|t|^\alpha\}, \tag{1}$$

where α ($0 < \alpha \leq 2$) is called the characteristic exponent. It measures the “thickness” of the tails of the distribution. The smaller is the value of α , the heavier are the tails. a is the location parameter determines the center of the $S\alpha S$ distribution. γ is the scale parameter, which is similar to the variance of the Gaussian distribution. The $S\alpha S$ distribution is symmetric about a . Gaussian distribution is a special case of the $S\alpha S$ distribution (i.e., when $\alpha = 2$). Usually there is no closed-form expressions for the general $S\alpha S$ density functions. But it can be satisfactorily approximated by power series expansions [6].

Figures 1(e) to 1(g) show the bested fitted $S\alpha S$ models obtained by using the maximum likelihood for various frequency bands. It is observed that the heavy-tailed behavior is well modeled. To further investigate the importance for the existence of heavy-tailed behavior, Figure 2 highlights the voxels, which lie on the smallest 10% or largest 10% of the energy magnitudes in various frequency bands with green circles. In Figure 2, the voxels highlighted with green circles cannot be satisfactorily modeled by Gaussian as they lie on the "tail" of the frequency magnitude histograms. It is observed that most of these voxels are located at salient regions, which are important for image registration, such as sulcal roots and gyral crowns [7]. Therefore, failure to model the heavy-tailed behavior satisfactorily can lead to significant loss of information and degrade the registration performance.

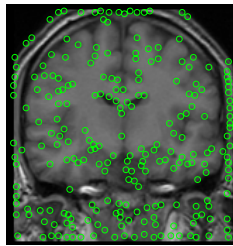


Fig. 2. Voxels highlighted with green circles are corresponding to the smallest 10% and largest 10% of the energy magnitudes in various frequency bands. They lie on the "tail" of the frequency magnitude histograms.

Table 1 lists the sums of squared errors of different frequency band magnitudes modeled by the Gaussian and $S\alpha S$ distributions. It is shown that the $S\alpha S$ distribution can model the energy magnitude distribution more accurately than the Gaussian distribution.

Table 1. Sums of squared errors of modeling the energy magnitude distribution using the Gaussian and $S\alpha S$ distributions for different frequency bands refer to Figure 1

	Low Frequency	Mid Frequency	High Frequency
<i>Gaussian</i>	0.3076	0.5308	0.4803
<i>SαS</i>	0.0107	0.0291	0.0134

Therefore, in this paper, we propose $S\alpha S$ filters as a new feature extraction method for brain MR images. A 3D $S\alpha S$ filter is defined as,

$$\psi_{\alpha,\gamma,f,\theta,\phi}(x, y, z) = f_{\alpha,\gamma}(x, y, z) \cdot \exp(j2\pi(xu + yv + zw)), \tag{2}$$

where $f_{\alpha,\gamma}(x, y, z)$ is the zero-mean $S\alpha S$ kernel and defined as,

$$f_{\alpha,\gamma}(x, y, z) = \left(\frac{1}{\sqrt{2\pi}}\right)^3 \int_u \int_v \int_w \exp\{-\gamma(x^2 + y^2 + z^2)^{\frac{\alpha}{2}}\} \cdot \exp(j(xu + yv + zw)) dw dv du. \tag{3}$$

In Equation 2, $u = f \cdot \sin \phi \cos \theta$, $v = f \cdot \sin \phi \sin \theta$, $w = f \cdot \cos \phi$ ($0 \leq \theta \leq \pi$, $0 \leq \phi \leq \pi$), where $f = \sqrt{u^2 + v^2 + w^2}$ is the center frequency, θ and ϕ define the orientations in the frequency domain. Gabor filter is a special case of $S\alpha S$ filters (i.e., when $\alpha = 2$).

During the feature extraction process, the input image is convolved with the $S\alpha S$ filters. Then the magnitudes of the filtered response are normalized to the range $[0,1]$ and adopted as the features. In this paper, the input image is convolved with a set of $S\alpha S$ filter banks with various characteristic exponents, center frequencies and orientations. The center frequencies and orientations are defined as, $f_i = f_{max}/(\sqrt{2})^i$ ($i = 0, 1, \dots, N_f$), $\theta_j = j\pi/N_\theta$ ($j = 0, 1, \dots, N_\theta$), $\phi_k = k\pi/N_\phi$ ($k = 0, 1, \dots, N_\phi$). N_f , N_θ and N_ϕ are the numbers of center frequencies and orientations to be decomposed in the 3D frequency domain, f_{max} is the highest center frequency to be analyzed. In this paper, $f_{max} = 16.00$ (cycles/image), $N_f = 5$, $N_\theta = 6$ and $N_\phi = 6$. Four different characteristic exponents are used to capture the heavy-tailed behavior: $\alpha_1 = 0.5$, $\alpha_2 = 1$, $\alpha_3 = 1.5$ and $\alpha_4 = 2$. The scale parameter γ is set for each filter so that each filter has a half peak radial bandwidth of one octave.

2.2 The Maximum Response Orientation Selection Criterion

As stated in Section 2.1, the $S\alpha S$ filters can capture the non-Gaussian heavy-tailed behavior. However, it is still not rotation invariant. As pointed out in [7], rotation invariance is an essential property for feature-based registration methods. As such, we propose the Maximum Response Orientation (MRO) selection criterion to make the filters rotation invariant. Suppose for a given characteristic exponent α and center frequency f , according to the formulation described in Section 2.1, there are $N_\theta \cdot N_\phi$ responses for each voxel with respect to different orientations. Then the maximum response for each voxel is defined as,

$$R(x, y, z) = \max_{j,k} |I * \psi_{\alpha,\gamma,f,\theta_j,\phi_k}(x, y, z)|, \quad (4)$$

where I denotes the input image, the $*$ symbol means convolution. As a result, the $R(x, y, z)$ value for each voxel is rotation invariant because no matter how the images are rotated, the maximum response value still maintains the same for a particular direction. Also, the feature dimension can be reduced significantly. Without the MRO selection criterion, each voxel is represented by a $4 * 5 * 6 * 6 = 720$ dimension feature vector (four characteristic exponents, five center frequencies, six θ directions and six ϕ directions). After applying the MRO selection criterion, the feature dimension is reduced to $4 * 5 * 1 * 1 = 20$. Therefore, the computational burden is remarkably reduced.

2.3 Training Option with Pre-obtained Segmentation Results

Sections 2.1 and 2.2 introduce the procedure for extracting features from brain MR images using $S\alpha S$ filters and the MRO selection criterion. It is an unsupervised process. In this section, we present a training framework if the segmentation results of the brain MR images are available before the registration.

Suppose the source image is denoted as G_s , and it is segmented into c classes of tissues. For each referencing voxel p , a sphere with radius R is defined whose origin is the referencing voxel. Then all the voxels on or inside this sphere are under consideration. R actually defines the maximum scale of the spherical neighborhood system, in this paper, $R = 3$. For all the voxels under consideration, let N_i ($i=1,2,\dots,c$) denote the number of voxels belong to the i -th tissue, $H_{i,j}^p$ denote the feature vector obtained using $S\alpha S$ filter banks and the MRO criterion from the j -th voxel of the i -th class. Then for each referencing voxel p , an appropriate weighting factor can be assigned to it using the Fisher's separation criterion (FSC) [9]. First, the intra-class mean and variance are calculated as,

$$m_I^p = \frac{1}{c} \sum_{i=1}^c \frac{2}{N_i(N_i - 1)} \sum_{k=2}^{N_i} \sum_{j=1}^{k-1} \chi^2(H_{i,j}^p, H_{i,k}^p), \tag{5}$$

$$\sigma_I^p = \left(\frac{2}{\left(\sum_{i=1}^c N_i(N_i - 1)\right) - 2} \sum_{i=1}^c \sum_{k=2}^{N_i} \sum_{j=1}^{k-1} \left(\chi^2(H_{i,j}^p, H_{i,k}^p) - m_I^p\right)^2 \right)^{\frac{1}{2}}. \tag{6}$$

Then the inter-class mean and variance are calculated as,

$$m_E^p = \frac{2}{c(c - 1)} \sum_{i=1}^{c-1} \sum_{j=i+1}^c \frac{1}{N_i N_j} \sum_{k=1}^{N_i} \sum_{l=1}^{N_j} \chi^2(H_{i,k}^p, H_{j,l}^p), \tag{7}$$

$$\sigma_E^p = \left(\frac{1}{\left(\sum_{i=1}^{c-1} \sum_{j=i+1}^c N_i N_j\right) - 1} \sum_{i=1}^{c-1} \sum_{j=i+1}^c \sum_{k=1}^{N_i} \sum_{l=1}^{N_j} \left(\chi^2(H_{i,k}^p, H_{j,l}^p) - m_E^p\right)^2 \right)^{\frac{1}{2}}, \tag{8}$$

where χ^2 denotes the *chi* square distance. Then the weighting factor for voxel p is given as,

$$w_p = \frac{(m_I^p - m_E^p)^2}{(\sigma_I^p)^2 + (\sigma_E^p)^2}. \tag{9}$$

Similar to the source image, each voxel of the target image can also be assigned an appropriate weighting factor using this training framework when the segmentation results are available.

3 Similarity Measure and Deformation Model

In this paper, the GSEE-MI [10] is adopted as the similarity measure. GSEE-MI is defined based on the multi-dimensional cumulative distribution function and therefore can be directly applied to the multi-dimensional features extracted from the proposed method. It is also less sensitive to interpolation effect. If the training option described in Section 2.3 is not used, then each voxel will have equal weight when calculating the cumulative distribution function. If the training option is adopted, then when calculating the cumulative distribution

function, each voxel contributes its weighting factor w_p for its corresponding histogram bin. Regarding the optimization, the gradient descent method is used. The gradient of GSEE-MI can be approximated by using the Richardson's extrapolation method [11]. The tri-cubic B-spline basis function is adopted as the deformation model for the proposed method in the non-rigid registration task, the control-point spacing was set at 2.5mm.

4 Experimental Results

4.1 Experiment with Simulated 3D Images

In this section, we have tested the performance of the proposed method upon the simulated 3D T1 image data obtained from the BrainWeb². 12 image volumes from different subjects were used. One of the image volumes was served as the reference image, the others were used as the target images. The image volume of each subject has the resolution of $256 \times 256 \times 181$ voxels with the tissues of different classes (i.e., white matter, gray matter and cerebrospinal fluid). From the BrainWeb, all voxels have been already segmented and labeled.

The evaluation method was based on the calculation of the overlap of gray matter (GM), white matter (WM) and cerebrospinal fluid (CSF) between the reference image and transformed target image [12]. The evaluation measure was defined by $P = \frac{N(A \cap B)}{N(A \cup B)}$ [12], where A and B denote the regions of a specific tissue in two images. The average values of P and the standard deviations of the GM, WM and CSF before registration, registration results obtained by using FFD [2], Demons [1], Gabor features [5] and the proposed method ($S\alpha S$) with and without training process are listed in Table 2. As listed in Table 2, the proposed method gives the highest values of P among all the compared methods for the registrations of the simulated 3D data sets. When the training procedure is adopted, the registration accuracy can be further improved.

Table 2. The mean values of P and SDs of the tissues of GM, WM and CSF with different methods. *BR* denotes before registration, *S α S (WOT)* denotes using *S α S* filters without training, *S α S (WT)* denotes using *S α S* filters with training.

Tissue	BR	FFD	Demons	Gabor	<i>SαS</i> (WOT)	<i>SαS</i> (WT)
Gray	0.43167±0.09	0.74934±0.04	0.77052±0.06	0.72563±0.08	0.82115±0.03	0.87832±0.04
White	0.45638±0.06	0.76042±0.02	0.77374±0.03	0.73093±0.05	0.81093±0.04	0.85129±0.06
CSF	0.35985±0.03	0.71524±0.04	0.73095±0.05	0.69442±0.02	0.78205±0.05	0.82903±0.02

4.2 Experiment on Real 3D Images

We have conducted a non-rigid registration experiment on real 3D T1-weighted brain MR data obtained from the IBSR website³. The experiment was performed

² <http://www.bic.mni.mcgill.ca/brainweb/>

³ <http://www.cma.mgh.harvard.edu/ibsr/index.html>

on 20 image volumes of different subjects. The image volume for each subject is around $256 \times 256 \times 64$ voxels. For each image, the ground truth of segmented tissues of different classes is available at the IBSR website. The experimental settings were similar to the experiments presented in Section 4.1. The value of P [12] was used to evaluate and compare between different methods. The experimental results are listed in Table 3. It is observed that in the real 3D data experiments, the proposed method has the highest values of P among all the compared methods. Therefore, the robustness and accuracy of the proposed method are strongly implied.

Table 3. The mean values of P and SDs of the GM, WM and CSF with different methods. BR denotes before registration, $S\alpha S$ (WOT) denotes using $S\alpha S$ filters without training, $S\alpha S$ (WT) denotes using $S\alpha S$ filters with training.

Tissue	BR	FFD	Demons	Gabor	$S\alpha S$ (WOT)	$S\alpha S$ (WT)
Gray	0.52456±0.05	0.73146±0.05	0.76883±0.03	0.72925±0.06	0.81525±0.05	0.85184±0.06
White	0.55185±0.03	0.77935±0.05	0.78105±0.01	0.75274±0.04	0.83902±0.03	0.86096±0.08
CSF	0.31868±0.04	0.73802±0.04	0.75023±0.03	0.70214±0.05	0.81935±0.04	0.84086±0.03

5 Conclusion

In this paper, a new non-rigid registration method is proposed and evaluated. The $S\alpha S$ filters are designed to model the non-Gaussian heavy-tailed behavior of the energy magnitude distributions of different frequency bands for brain MR images. The maximum response orientation (MRO) selection criterion is proposed to make the extracted features rotation invariant and reduce computational burden. A new training framework based on the Fisher's separation criterion (FSC) is provided if the segmentation results for the source and target images are available. The proposed method has been compared with the free-form deformation based method, Demons algorithm and a method using the Gabor features. It is shown that the proposed method achieves the highest registration accuracy in the experiments on both simulated and real 3D IBSR data sets.

References

1. Thirion, J.: Image matching as a diffusion process: an analogy with maxwell's demons. *MedIA* 2, 243–260 (1998)
2. Rueckert, D., Sonoda, L., et al.: Nonrigid registration using free-form deformations: Application to breast MR images. *TMI* 18, 712–721 (1999)
3. Vemuri, B., Ye, J., et al.: A level-set based approach to image registration. In: *MMBIA*, pp. 86–93 (2000)
4. Maintz, J., Viergever, M.: A survey of med. image registration. *MedIA* 2(98), 1–36
5. Liu, J., Vemuri, B., Marroquin, J.: Local frequency representations for robust multimodal image registration. *TMI* 21, 462–469 (2002)
6. Nikias, C., Shao, M.: *Signal Processing with Alpha-Stable Distributions and Applications*. Wiley, Chichester (1995)

7. Shen, D., Davatzikos, C.: HAMMER: Hierarchical attribute matching mechanism for elastic registration. *TMI* 21, 1421–1439 (2002)
8. Gabor, D.: Theory of communication. *IEEE Journal of Institute of Electrical Engineers* 93, 429–457 (1946)
9. Parry, R., Essa, I.: Feature weighting for segmentation. In: *ICMIR*, pp. 116–119 (2004)
10. Liao, S., Chung, A.: Multi-modal image registration using the generalized survival exponential entropy. In: Larsen, R., Nielsen, M., Sporring, J. (eds.) *MICCAI 2006*. LNCS, vol. 4191, pp. 964–971. Springer, Heidelberg (2006)
11. Mathews, J., Fink, K.: *Numerical Methods Using MATLAB*. Pearson, London (2004)
12. Crum, W., Rueckert, D., et al.: A framework for detailed objective comparison of non-rigid registration algorithms in neuroimaging. In: Barillot, C., Haynor, D.R., Hellier, P. (eds.) *MICCAI 2004*. LNCS, vol. 3216, pp. 679–686. Springer, Heidelberg (2004)